AJNR Am J Neuroradiol 21:1078–1083, June/July 2000

Diffusion Changes in the Aging Human Brain

Terry Chun, Christopher G. Filippi, Robert D. Zimmerman, and Aziz M. Uluğ

BACKGROUND AND PURPOSE: **Quantifying changes in the human brain that occur as part of normal aging may help in the diagnosis of diseases that affect the elderly and that cause structural changes in the brain. We sought to assess diffusion changes that are inherently related to brain structure during aging.**

METHODS: **MR scans were obtained from 11 healthy volunteers and 27 patients (ages 26 to 86 years [53.4 ± 17.0 years]). Images acquired from the patients either showed no abnormalities, contained minimal periventricular white matter changes, or revealed focal lesions. Maps of the average diffusion constant (D_{av}) were calculated for each subject. Changes in D_{av} were determined with distribution analysis (histogram) for the entire brain and compared with region-of-interest measurements from the periventricular white matter and thalamus.**

RESULTS: **Mean D_{av} of the entire brain ($0.74 \pm 0.02 \times 10^{-5}$ cm^2/s) showed weaker age dependency compared with the periventricular white matter D_{av}($0.76 \pm 0.04 \times 10^{-5}$ cm^2/s). The D_{av} of the thalamus D_{av} ($0.75 \pm 0.03 \times 10^{-5}$ cm^2/s) had no age dependency. The age-dependent changes of entire brain D_{av} may be significant for subjects older than 60 years compared with younger subjects.**

CONCLUSION: **In this study, we observed minimal changes in the D_{av} of the entire brain with aging. The mean D_{av} of the human brain is nearly constant throughout most of adulthood.**

Changes in brain structure are a normal aspect of aging and are well documented with MR studies (1–3). The most notable changes observed in the elderly include enlargement of CSF spaces, hyperintense regions in the white matter and basal ganglia, and widening of cortical sulci associated with brain atrophy (1, 2). Images obtained with standard MR protocols are effective for evaluating these gross anatomic changes, but few microstructural alterations can be inferred with this method.

Recently, age-related brain changes have been assessed with MR diffusion imaging (4–6). This method is sensitive to incoherent water motion, which is dependent on the brain's microstructure. In 1994, Gideon and colleagues (4) indicated a positive correlation between the diffusion constant of white matter and aging. They speculated that these changes may be caused by age-dependent neuronal degeneration or by changes in myelination. Their study, however, required electrocardiographic triggering to avoid influences of pulsatile brain motion and was limited to diffusion measurements in one direction only. That same year, Nomura and colleagues (5) reported diffusion constants that were fairly unchanged in adults. That study measured diffusion constants in two directions and focused mostly on the diffusion differences between pediatric and adult subjects. More recently, Nusbaum and colleagues (6) reported their preliminary data during a conference on diffusion changes in cerebral white matter revealed by echo-planar fluid-attenuated inversion-recovery tensor imaging. They showed that histograms of the orientation-independent diffusion tensor trace can be used to assess whole-brain changes in diffusion.

The purpose of our study was to evaluate age-related changes in brain diffusion and provide age-specific normative values, which may serve as a baseline for future research.

Methods

Our subjects included 11 healthy volunteers and 27 patients. Imaging examinations of 15 patients and 11 volunteers showed no abnormalities. Examinations in nine patients showed minimal periventricular white matter ischemic changes (less than five small focal regions, each). One patient's examination revealed a small chronic cerebellar infarct, one patient had an infarct in the pons, and one had a small thalamic lacunar infarct. For the purposes of our study, the positive findings listed above (12 subjects out of 38) should not have affected our measurements because they were very small and localized. The age range of the subjects was 26 to 86 years, with a mean of

Received August 20, 1999; accepted after revision January 24, 2000.

From the Weill Medical College of Cornell University—New York Presbyterian Hospital, Department of Radiology, 1300 York Avenue, New York, New York.

Address reprint requests to Aziz M. Uluğ, PhD, Weill Medical College of Cornell University, Department of Radiology, Box 141, 1300 York Avenue, New York, NY 10021.

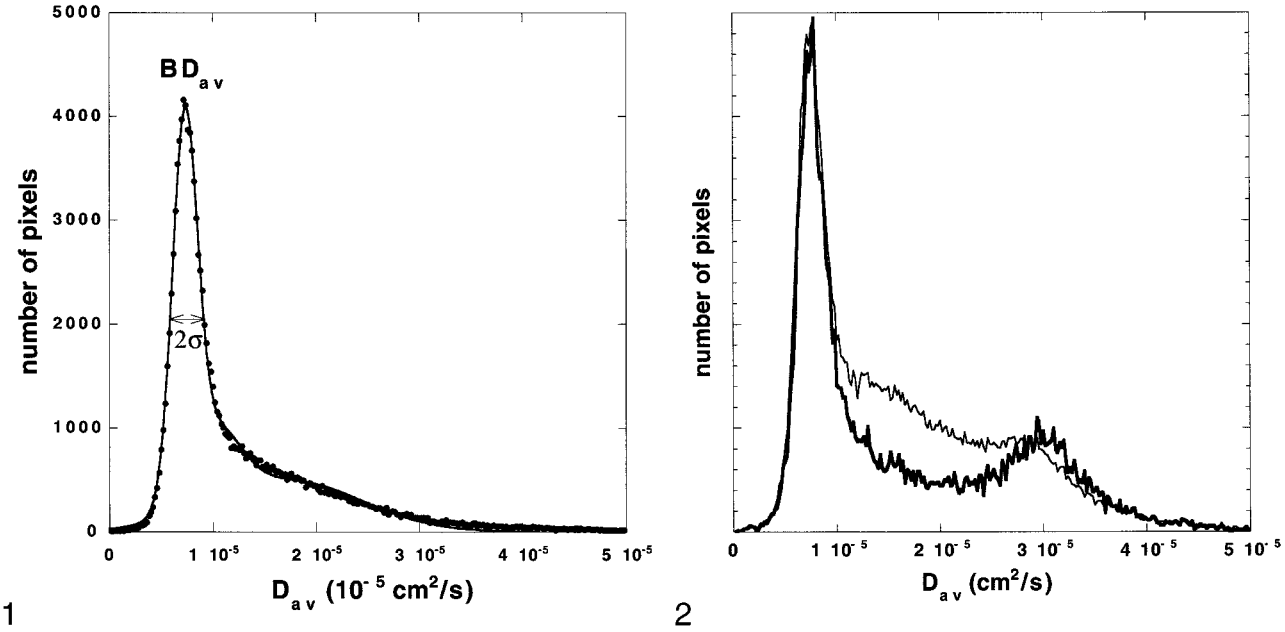

FIG 1. Whole-brain–diffusion-constant distribution map (diffusion histogram) from a healthy volunteer. The data (*dots*) are fitted with a triple gaussian function to accommodate the two-compartment nature of the data and the mixing between two compartments (*solid curve*). The brain tissue compartment has a narrow distribution of values around its mean. The second and third compartments have broader distributions. The mean of the brain tissue pixel distribution (also mode of the entire distribution) is recognized as a mean diffusion constant for the entire brain (BD_{av}). The distribution width (σ) of the brain tissue compartment is also recorded.

FIG 2. BD_{av} histograms from an 86-year-old subject with age-appropriate atrophy. The thicker curve is the D_{av} histogram from three slices through the lateral ventricles. The tissue peak (around 0.75×10^{-5} cm²/s) and the CSF peak (around 3.2×10^{-5} cm²/s) are well separated. The thinner curve is the whole-brain D_{av} histogram. The location of the tissue peaks in both histograms did not change, demonstrating that the tissue peak is truly free of CSF contamination. The histograms are scaled so that the tissue peaks are the same height.

53.4 years and standard deviation of 17.0 years. This group included 20 male and 18 female subjects.

MR scans were acquired for all subjects on a 1.5-T scanner. Axial diffusion images (10 000/100 [TR/TE]; FOV, 22 cm; 30 interleaved slices of 5-mm thickness; image matrix, 128×128) were obtained with an echo-planar multislice sequence. Diffusion was measured in three directions (x, y, z), with a b-value of 100 000 s/cm² for each direction. In addition, an image without diffusion gradients was acquired. Using diffusion-weighted images in three orthogonal directions, an orientation-independent diffusion-weighted image (DWI_{trace}), which is related to the trace of the diffusion tensor, is obtained on the scanner as follows: $DWI_{trace} = \sqrt[3]{DWI_x \, DWI_y \, DWI_z}$. This trace-weighted image and the image without diffusion weighting (S_o) is transferred to a computer workstation. A C program employing the equation ($DWI_{trace} = S_o \exp(-bD_{av})$) is used to calculate the orientation-independent average diffusion maps (D_{av} = Trace/3) on a pixel-by-pixel basis.

Another custom C program was then used to calculate the diffusion distribution maps (histograms) from the entire brain (BD_{av}) (Fig 1). The program distributed the pixels to 250 bins with bin widths of 0.02×10^{-5} cm²/s. This distribution map (histogram) was fitted to a triple gaussian curve using commercial software (KaleidaGraph, Adelbeck Software, Reading, PA). This curve

$$(C_1 e^{-[(D_{av}-BD_{av})/\sigma]^2} + C_2 e^{-[(D_{av}-D_2)/\sigma_2]^2} + C_3 e^{-[(D_{av}-D_3)/\sigma_3]^2})$$

represents a two-compartment model with mixing (three compartments): 1) the brain tissue compartment, 2) brain tissue mixed with CSF, and 3) the high-diffusion compartment consisting of CSF and non-brain tissue, such as the eyeballs. Peak locations and peak widths were determined from the fitted data. The peak location of the tissue compartment (mode of the entire distribution and the median of the tissue pixels) was interpreted to be BD_{av}. We also measured the tissue-compartment D_{av} distribution width, σ. Because the diffusion constant of CSF is more than four times higher than that of the brain tissue, the tissue pixels contaminated with more than 10% CSF would be included in the broad mixing compartment. Hence, the measured BD_{av} and σ characterize the brain tissue pixels that are not contaminated with CSF (Fig 2).

We also measured the D_{av} values of the periventricular white matter and thalamus by using region-of-interest (ROI) analysis. We used a custom program (IMAX2, courtesy of Dr. Peter Barker, Johns Hopkins University). This program allows placement of ROIs on D_{av} maps and calculates the mean value for each ROI. Periventricular white matter measurements included 16 to 38 ROIs placed over three slices for 36 subjects and over two slices for two subjects. Thalamic measurements included two ROIs placed on a single slice.

To compare the D_{av} measurements between different patient age groups, we used a two-tailed Student's *t*-test. Pearson correlation coefficients were calculated with commercial software (KaleidaGraph). The significance level was set at $P < .05$.

Results

Our study population consisted of 38 subjects with an age range of 26 to 86 years and a mean age of 53.4 ± 17.0 years. For all subjects, our distribution analysis showed the mean BD_{av} to be 0.74×10^{-5} cm²/s, with a standard deviation of 0.02×10^{-5} cm²/s. The ROI measurements showed that the periventricular white matter D_{av} was $0.76 \pm 0.04 \times 10^{-5}$ cm²/s and the thalamus D_{av} was 0.75

TABLE 1: Average diffusion measurements for the study population (n = 38) (age range 26–86 years, mean 53.4 ± 17.0 years)

BD_{av}	$0.74 \pm 0.02 \times 10^{-5}$ cm^2/s
σ	$0.18 \pm 0.01 \times 10^{-5}$ cm^2/s
Periventicular white matter D_{av}	$0.76 \pm 0.04 \times 10^{-5}$ cm^2/s
Thalamus D_{av}	$0.75 \pm 0.03 \times 10^{-5}$ cm^2/s

Note.—Values reported as mean ± standard deviation. BD_{av} is the mean average diffusion constant for the brain; σ is distribution width of brain tissue average diffusion constant.

$\pm 0.03 \times 10^{-5}$ cm^2/s (Table 1). These findings are in excellent agreement with previously reported values (4, 7–11).

On inspection (Fig 3), BD_{av} increases gradually with age ($r = 0.383$, $P < .05$), but this age dependency is minimal (4.21×10^{-9} cm^2/s per year). In contrast, the periventricular white matter D_{av} (Fig 4) measurements, which were obtained by ROI placement, were more significantly correlated with age ($r = 0.406$, $P < .05$), with an age-dependency factor of 8.76×10^{-9} cm^2/s per year. No correlation was seen between thalamic D_{av} and age (Fig 5) ($r = 0.174$, $P > .29$), which was also measured by ROI placement.

When evaluating BD_{av} changes, we observed a statistically significant difference ($P < .05$) when we compared subjects 60 years or older with subjects younger than this (Table 2). For the subjects in the age range of 60 to 86 years, the BD_{av} was $0.75 \pm 0.01 \times 10^{-5}$ cm^2/s, whereas for the younger population, this value was $0.74 \pm 0.02 \times 10^{-5}$ cm^2/s. Similarly, the D_{av} for periventricular white matter was also significantly different between these two groups. This value was calculated to be $0.78 \pm 0.04 \times 10^{-5}$ cm^2/s for the older population and $0.76 \pm 0.03 \times 10^{-5}$ cm^2/s for the younger group. There was no significant difference in measurement of the thalamus between these two age groups.

When we divided the study population into three equal groups (ages 26–45 years, n=13; 46–59 years, n=12; and 60+ years, n=13), we observed a highly significant difference only in the periventricular white matter D_{av} ($P < .009$) and BD_{av} ($P < .003$) of the youngest and oldest groups (Table 3).

There were no statistically significant changes with age for the D_{av} distribution width, σ (Fig 6) ($r = 0.273$, $P > .1$). For the entire adult population, the D_{av} distribution width, σ, was measured to be $0.18 \pm 0.01 \times 10^{-5}$ cm^2/s.

Discussion

Diffusion imaging is being used with increasing frequency in a large number of clinical and experimental circumstances. On scanners equipped with high-speed gradient systems, diffusion imaging can be performed in less than 1 minute and immediately displayed without the need for off-line processing. Because of this speed, ease of performance, and utility in the detection of pathologic processes, particularly in the detection of acute infarction, diffusion imaging has become a routine component of brain MR imaging protocols at many institutions. These clinical images are an enormous potential resource for the quantitative scientific investigation

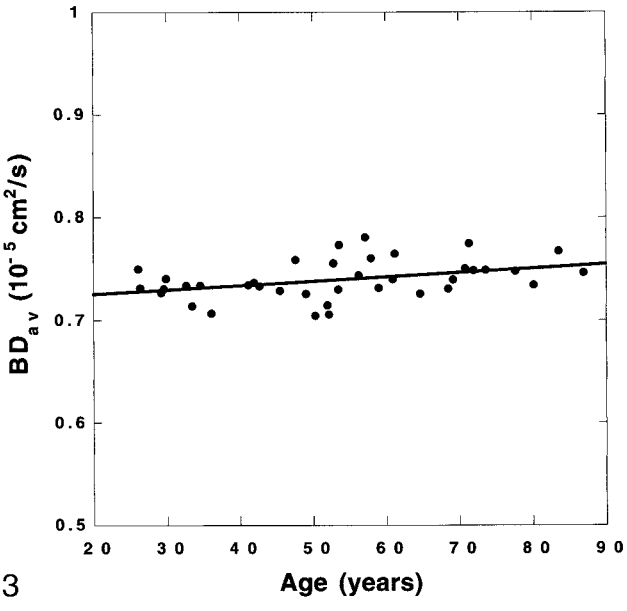

3

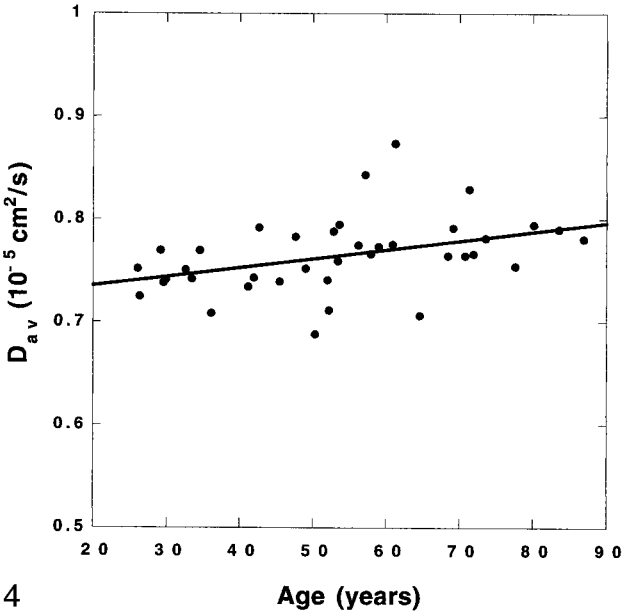

4

FIG 3. The brain diffusion constants (*circles*) measured from distribution maps are plotted against age of the subjects. A linear fit to the data (*solid line*) is also shown ($BD_{av} = 0.717 + 0.000421 \times$ Age, $r = 0.383$, $P < .05$). Age dependency of the data is minimal.

FIG 4. The diffusion constants determined from ROI measurements of the periventricular white matter (*circles*) are plotted against age of the subjects. There is a significant increase with respect to age. A linear fit to the data (*solid line*) is also shown ($D_{av} = 0.718 + 0.000876 \times$ Age, $r = 0.406$, $P < .015$).

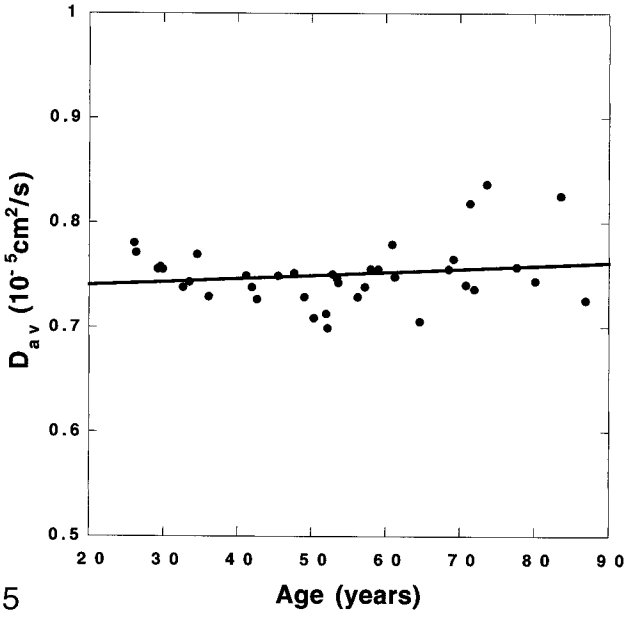

5

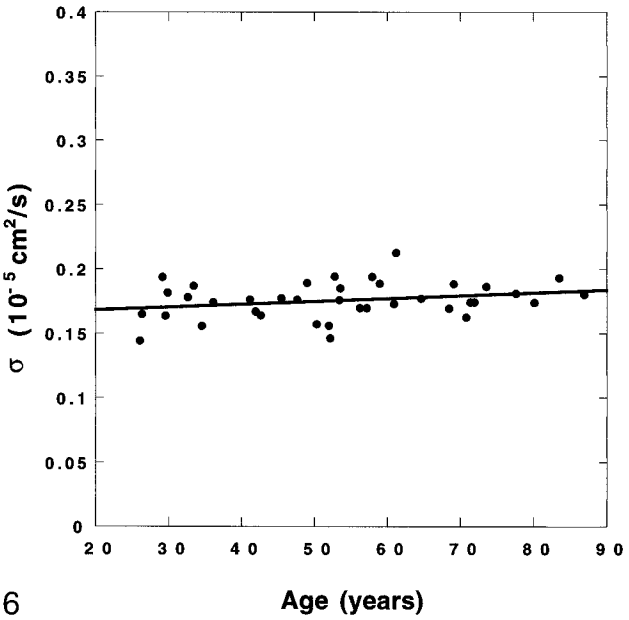

6

FIG 5. The diffusion constants measured from the thalamus (*circles*) by using ROIs are plotted against age of the subjects. Data do not show age dependency. A linear fit to data (*solid line*) is also shown (D_{av} = 0.734 + 0.000301 × Age, r = 0.174, $P > .29$).

FIG 6. The distribution width (σ) of the brain diffusion constants measured from distribution maps (*circles*) are plotted against age of the subjects. Data do not show age dependency. A linear fit to the data (*solid line*) is also shown (σ = 0.163 + 0.000227 × Age, r = 0.274, $P > .10$).

TABLE 2: Average diffusion measurements between subjects 60+ years and subjects younger than 60 years

Age Group	< 60 Years	60+ Years	Significance
Mean age	43.6 ± 10.9 years	72.3 ± 8.0 years	
	n = 25	n = 13	
BD_{av}	0.74 ± 0.02 × 10^{-5} cm^2/s	0.75 ± 0.01 × 10^{-5} cm^2/s	$P < .05$
Periventricular white matter D_{av}	0.76 ± 0.03 × 10^{-5} cm^2/s	0.78 ± 0.04 × 10^{-5} cm^2/s	$P < .05$
Thalamus D_{av}	0.74 ± 0.02 × 10^{-5} cm^2/s	0.76 ± 0.04 × 10^{-5} cm^2/s	Not significant

Note.—Values reported as mean ± standard deviation.

TABLE 3: Average diffusion measurements of three age groups

Age Group	26–45 Years	46–59 Years	60+ Years
Mean age	34.1 ± 6.5 years	53.4 ± 3.6 years	72.3 ± 8.0 years
	n = 13	n = 12	n = 13
BD_{av}	0.73 ± 0.01 × 10^{-5} cm^2/s	0.74 ± 0.03 × 10^{-5} cm^2/s	0.75 ± 0.01 × 10^{-5} cm^2/s
Periventricular white matter D_{av}	0.75 ± 0.02 × 10^{-5} cm^2/s	0.76 ± 0.04 × 10^{-5} cm^2/s	0.78 ± 0.04 × 10^{-5} cm^2/s
Thalamus D_{av}	0.75 ± 0.02 × 10^{-5} cm^2/s	0.74 ± 0.02 × 10^{-5} cm^2/s	0.76 ± 0.04 × 10^{-5} cm^2/s

Note.—Values reported as mean ± standard deviation.

of the normal and pathologic states of the brain. Diffusion-weighted sequences are sensitive to microscopic movement of water molecules; therefore, alterations in degree of diffusion reflect alteration in the microscopic environment of these water molecules. It is, therefore, reasonable to infer that changes in diffusion reflect changes at the scale of cellular and extracellular structures of the brain.

In this study, we assessed the diffusion characteristics of the entire brain as a function of age by using data obtained from a routine diffusion-weighted sequence widely used in clinical practice. This knowledge is important for two reasons:

i. The identification of changes in diffusion in otherwise normal-appearing brain can increase our understanding of the normal processes of aging. Previous investigators have shown that the diffusion within the maturing brain is age-dependent (5). In children under

2 years of age, diffusion is increased compared with older children and adults. This difference has been ascribed to the lack of or incomplete myelination, with consequent increased water motion relative to the more restrictive environment seen in fully mature, myelinated brain. Prior published studies have also suggested that diffusion increases in the elderly (4). These early investigations were limited by technical factors. They were performed using diffusion-sensitizing gradients in only one or two directions; thus, white matter diffusion anisotropy effects could not be eliminated or evaluated independently. In addition, the entire brain was not imaged.

ii. The knowledge of age-dependent normal diffusion values is critical in the assessment of diffuse processes such as hypertensive encephalopathy (due to vasogenic edema) and obstructive hydrocephalus (due to interstitial edema) (12, 13). Changes in diffusion have been assessed by obtaining multiple ROI measurements from locations in the brain. This technique is limited for several reasons. The choice of location, number, and size of ROIs is operator dependent. This may lead to site-selection bias and may limit the reproducibility of results. ROIs may include heterogeneous tissues (eg, white matter and CSF) and measurements of diffusion may fail to reveal changes occurring in the brain tissue.

The use of distribution analysis of average diffusion constant (D_{av} histograms) provides an effective method for measuring mean diffusion for the entire brain. The three-dimensional diffusion information of a subject's brain can be reduced to a single number (mean brain diffusion constant: BD_{av}) by using appropriate modeling. This physical parameter can be used for intersubject comparison. Furthermore, because this is an automated process, no operator bias can interfere with the determination of BD_{av}. ROI measurements, on the other hand, depend on correct identification of the measured structure by the operator. Also, because signal-to-noise ratio in a given measurement is proportional to the square root of the number of pixels measured, the determination of BD_{av} is much more precise than a given ROI measurement. The distribution analysis uses all pixels, whereas ROI measurement uses only the pixels of interest. The standard deviations of measurements in Table 1 confirm this fact. The standard deviation of BD_{av} measurements is the lowest when compared with the standard deviations of the thalamus and the periventricular white matter D_{av} measurements.

The use of distribution analysis has other advantages. Distributing pixels according to signal intensity theoretically should remove the contaminating effects of blood vessel flow and small CSF spaces (lacunes and Virchow-Robin spaces). On D_{av} maps, these phenomena appear as foci of high diffusion. These regions may be unintentionally included in ROI measurements, causing abnormal elevation of D_{av} values. Histograms distribute the pixels of these high-diffusion areas to the right and remove their contribution to brain tissue D_{av} measurements.

Our analysis showed that D_{av} in brain tissue has a gaussian distribution. This is expected for the brain, which has a relatively homogeneous distribution of tissue water. Furthermore, the D_{av} distribution width was not correlated with age (Fig 5), indicating that the brain water distribution does not change considerably during normal aging.

In this study, BD_{av} was found to be nearly constant. The BD_{av} measurements obtained from different healthy subjects of different ages were very close to each other. All the BD_{av} data measured were narrowly distributed between 0.70 and 0.78 10^{-5} cm^2/s. Significant changes with age were found only when the data of subjects older than age 60 years were compared with those of younger subjects.

The diffusion of water molecules in the human brain is restricted by the tissue microstructure. An increase in diffusion may be caused by either decreased restriction or increased water content. Evidence of changes in brain tissue microstructure during aging may come from a study done by Huttenlocher (14), who measured synaptic density in the human frontal cortex. Using a tissue-fixative method that revealed synaptic profiles, he showed that synaptic density was constant throughout most of adulthood (ages 16–72 years). There was, however, a small decline in synaptic density for the aged (ages 74–90 years). A decrease in synaptic density can reduce the restriction of water molecules and, hence, cause increased diffusion. Nonetheless, a homogeneous increase of brain tissue water with aging can also have the same effect.

White matter atrophy has been documented to occur with normal aging (1, 15–21). These changes are attributed to fiber degeneration, subcortical infarction, increasing Virchow-Robin spaces, and capillary changes in the blood-brain barrier (15–21). In our ROI measurements, which may be prone to the effects described above, we observed a statistically significant increase in the periventricular white matter D_{av} with age, but the thalamus D_{av} showed no age correlation. These trends agree with Gideon et al (4), who previously reported a positive correlation between white matter D_{av} and age but no significant age-related change in thalamic D_{av}. A study done by Miller et al (15) in 1980 also reports similar findings. Using an image analyzer, they showed an age-related increase in the gray matter:white matter ratio in subjects 50 years or older, suggesting that white matter loss occurs more rapidly after this age. Large Virchow-Robin spaces have been associated with age, hypertension, dementia, and incidental white matter lesions (20). These CSF-filled spaces accompany blood vessels penetrating the brain parenchyma, and are regarded as extensions of the subarachnoid space.

Because the subarachnoid space enlarges in the aging atrophic brain, the Virchow-Robin spaces may enlarge as well. Enlargement of these perivascular spaces in white matter can lead to increased free water diffusion and to increased white matter D_{av} measurements when ROIs are used.

Alternatively, increase in diffusion constant of white matter can be explained by increased water content caused by thinning blood vessels. In 1987, Stewart and colleagues (21) reported capillary changes in the blood-brain barrier in the aging human brain. In their study of biopsy specimens, they observed that white matter capillary walls become thinner as one ages. This thinning is caused by loss of pericytes and shrinkage of the endothelial cytoplasm. Loss of pericytes implies that the blood-brain barrier of the elderly is less efficient in preventing transient leaks. This may further increase white matter D_{av} measurements. If, however, this were the cause of the increase in ROI measurements of white matter diffusion constant, we would expect that the σ of the brain tissue should also change with age. We did not observe any statistical changes of σ during aging in this sample size, suggesting the water distribution of the brain tissue does not change during most of the adulthood.

We have provided a database of age-specific diffusion values of the periventricular white matter, thalamus, and the entire brain that can be used as normative values. We have shown in this study that distribution analysis can be used to assess whole-brain diffusion accurately. The contaminating effects from blood vessels and small fluid spaces are essentially eliminated, allowing for true measurements of the tissue diffusion constant. Further development in this methodology will likely increase its use for evaluating a number of brain diseases.

Conclusion

We have used data obtained from a routine clinical diffusion-weighted sequence to assess total brain diffusion. Distribution analysis and modeling were used to determine mean diffusion constant for the entire brain. The mean diffusion constant of the human brain is nearly constant throughout most of adulthood. Mild increase in the BD_{av} with age might be significant for individuals 60 years or older compared with younger subjects. Measurements from the periventricular white matter and thalamus obtained using ROIs showed an age-dependent increase in D_{av} of the periventricular white matter, but no changes in the thalamus.

Acknowledgments

We would like to thank Dr. Peter Barker of Johns Hopkins University for providing the IMAX2 data display and processing program that we used in ROI measurements. We would also like to thank the MR technologists (Richard Fischer, Sean Skolkin, John Crespo, John McCormick, Chul Gil Lee, Keith Clay, Thomas Farrell) at New York Presbyterian Hospital for their help with data transfers.

References

1. Drayer BP. **Imaging of the aging brain. Part I. Normal findings.** *Radiology* 1988;166:785–796
2. Jernigan TL, Press GA, Hesselink JR. **Methods for measuring brain morphologic features on magnetic resonance images. Validation and normal aging.** *Arch Neurol.* 1990;47:27–32
3. Pfefferbaum A, Mathalon DH, Sullivan EV, Rawles JM, Zipursky RB, Lim KO. **A quantitative magnetic resonance imaging study of changes in brain morphology from infancy to late adulthood.** *Arch Neurol.* 1994;51:874–887
4. Gideon P, Thomsen C, Henriksen O. **Increased self-diffusion of brain water in normal aging.** *JMRI* 1994;4:185–188
5. Nomura Y, Sakuma H, Takeda K, Tagami T, Okuda Y, Nakagawa T. **Diffusional anisotropy of the human brain assessed with diffusion-weighted MR: relation with normal brain development and aging.** *AJNR Am J Neuroradiol* 1994;15:231–238
6. Nusbaum AO, Tang CY, Buchsbaum MS, Wei TC, Atlas SW. **Global changes in cerebral white matter diffusion in normal aging.** *Proc Intl Soc Magn Reson Med* 1999;7:637
7. Uluğ AM, van Zijl PCM. **Orientation-independent diffusion imaging without tensor diagonalization: anisotropy definitions based on physical attributes of the diffusion ellipsoid.** *J Magn Reson Imaging* 1999;9:804–813
8. Chun T, Uluğ AM, van Zijl PCM. **Single-shot diffusion-weighted trace imaging on a clinical scanner.** *MRM* 1998;40:622–628
9. Pierpaoli C, Jezzard P, Basser PJ, Barnett A, Di Chiro G. **Diffusion tensor MR imaging of the human brain.** *Radiology* 1996; 201:637–648
10. Hirsch JG, Bock M, Essig M, Schad LR. **Comparison of diffusion anisotropy measurements in combination with the flair-technique.** *Magn Reson Imaging* 1999;17:705–716
11. Hajnal JV, Doran M, Hall AS, et al. **MR imaging of anisotropically restricted diffusion of water in the nervous system: technical, anatomic and pathologic considerations.** *J Comput Assist Tomogr* 1991;15:1–18
12. Gideon P, Thomsen C, Gjerris F, Sorensen PS, Henriksen O. **Increased self-diffusion of brain water in hydrocephalus measured by MR imaging.** *Acta Radiologica* 1994;35:514–519
13. Uluğ AM, Filippi CG, Souweidane M, Zimmerman RD. **Use of diffusion imaging for assessing the treatment of obstructive hydrocephalus.** *Proc Int Soc Magn Reson Med* 1999;7:1809
14. Huttenlocher PR. **Synaptic density in human frontal cortex—developmental changes and effects of aging.** *Brain Research* 1979;163:195–205
15. Miller AKH, Alston RL, Corsellis JAN. **Variation with age in the volumes of grey and white matter in the cerebral hemispheres of man: measurements with an image analyser.** *Neuropathol Appl Neurobiol* 1980;6:119–132
16. Awad IA, Spetzler RF, Hodak JA, et al. **Incidental subcortical lesions identified on magnetic resonance imaging in the elderly. I. Correlation with age and cerebrovascular risk factors.** *Stroke* 1986;17:1084–1089
17. Awad IA, Johnson PC, Spetzler RF, et al. **Incidental subcortical lesions identified on magnetic resonance imaging in the elderly. II. Postmortem pathological correlations.** *Stroke* 1986;17:1090–1097
18. Marshall VG, Bradley WG Jr., Marshall CE, Bhoopat T, Rhodes RH. **Deep white matter infarction: correlation of MR imaging and histopathologic findings.** *Radiology* 1988;167:517–522
19. Brant-Zawadzki M, Fein G, Van Dyke C, Kiernan R, Davenport L, de Groot J. **MR imaging of the aging brain: patchy white-matter lesions and dementia.** *AJNR Am J Neuroradiol* 1985;6: 675–682
20. Heier LA, Bauer CJ, Schwartz L, Zimmerman RD, Morgello S, Deck MDF. **Large virchow-robin spaces: MR-clinical correlation.** *AJNR Am J Neuroradiol* 1989;10:929–936
21. Stewart PA, Magliocco M, Hayakawa K, et al. **A quantitative analysis of blood-brain barrier ultrastructure in the aging human brain.** *Microvascular Research* 1987;33:270–282